Deterministic and cascadable conditional phase gate for photonic qubits

Citation	Chudzicki, Christopher, Isaac L. Chuang, and Jeffrey H. Shapiro. "Deterministic and cascadable conditional phase gate for photonic qubits." Phys. Rev. A 87, 042325 (April 2013). © 2013 American Physical Society
As Published	http://dx.doi.org/10.1103/PhysRevA.87.042325
Publisher	American Physical Society
Version	Final published version
Citable link	http://hdl.handle.net/1721.1/88739
Terms of Use	Article is made available in accordance with the publisher's policy and may be subject to US copyright law. Please refer to the publisher's site for terms of use.

Deterministic and cascadable conditional phase gate for photonic qubits

Christopher Chudzicki,[1,2] Isaac L. Chuang,[1,2] and Jeffrey H. Shapiro[2]

[1]*Department of Physics, Massachusetts Institute of Technology, Cambridge, Massachusetts 02139, USA*
[2]*Research Laboratory of Electronics, Massachusetts Institute of Technology, Cambridge, Massachusetts 02139, USA*

Previous analyses of conditional φ_{NL}-phase gates for photonic qubits that treat cross-phase modulation (XPM) in a causal, multimode, quantum field setting suggest that a large ($\sim\pi$ rad) nonlinear phase shift is always accompanied by fidelity-degrading noise [J. H. Shapiro, Phys. Rev. A **73**, 062305 (2006); J. Gea-Banacloche, *ibid.* **81**, 043823 (2010)]. Using an atomic $\vee$ system to model an XPM medium, we present a conditional phase gate that, for sufficiently small nonzero φ_{NL}, has high fidelity. The gate is made cascadable by using a special measurement, i.e., principal-mode projection, to exploit the quantum Zeno effect and preclude the accumulation of fidelity-degrading departures from the principal-mode Hilbert space when both control and target photons illuminate the gate. The nonlinearity of the $\vee$ system we study is too weak for this particular implementation to be practical. Nevertheless, the idea of cascading through principal-mode projection is of potential use to overcome fidelity-degrading noise for a wide variety of nonlinear optical primitive gates.

I. INTRODUCTION

In optical quantum logic, qubit states are usually encoded using the presence or absence of a single photon in one of the many modes of the quantum electromagnetic field. We refer to this special information-carrying mode as the *principal mode*. Logic gates can be high-fidelity only if they map input principal modes to output principal modes. Gates can be cascaded successfully if the input and output principal modes are the same. In either the dual-rail [1] or polarization [2] architectures, high-fidelity, cascadable single-qubit gates can be readily implemented using linear optics (beam splitters and phase shifters). A significant challenge to implementing optical quantum information processing is the faithful realization of a deterministic and cascadable universal two-qubit photonic logic gate.

Cross-phase modulation (XPM)—a nonlinear process in which one electric field affects the refractive index seen by another—has often been proposed [1,3–5] as a nonlinear optical process that might be used to construct such a universal gate, i.e., the conditional π-phase gate. (Other fundamentally different photonic two-qubit gates have been designed, e.g., [6,7], which involve only single-photon+atom interactions; such gates will not be discussed here.) While a single-mode analysis of XPM-based gates is encouraging, in recent years multimode efforts [8–10] that treat photons as excitations of a quantum field with continuously many degrees of freedom have been somewhat more foreboding.

In [8,9], the problem was studied using a quantized version of the solution to the classical coupled-mode equations for XPM. The XPM material was required to have a noninstantaneous response, as an instantaneous response in the quantum theory does not reproduce classical behavior for coherent-state mean fields. It was then shown that if the material response is noninstantaneous and causal, then noise terms necessary to preserve commutation relations cause the error probability (infidelity) $|\varepsilon|^2$ of conditional φ_{NL}-phase gates to be prohibitively large when $\varphi_{\mathrm{NL}} \sim \pi$. (See [10] for a comparative model study and [11] for experimental observation of this noise in optical fiber.)

A second difficulty with XPM is obtaining a cross-phase shift uniformly distributed over the control and target pulse profiles. Several authors have proposed conditional phase gate designs that avoid this trouble by allowing one pulse to propagate through the other [12–18]. As some point out [12], however, it is not clear that realizations of these proposals would be free from the causality-induced phase noise discussed above.

In the present paper, we offer a different approach to solving problems associated with quantum XPM. Rather than trying to achieve a high-fidelity π-phase shift all at once, we show that a high-fidelity conditional φ_{NL}-phase gate can be constructed for *small* φ_{NL}, and that these gates can be cascaded to yield a significant nonlinear phase shift with high fidelity. Indeed, showing that a conditional phase gate can be constructed with small nonlinear phase much larger than its error probability, $|\varepsilon|^2 \ll \varphi_{\mathrm{NL}} \ll 1$, is relatively easy. Cascading these gates, however, is nontrivial. The error, which results from a slight deformation of the principal modes, can be coherently amplified as the gate is cascaded, preventing the straightforward construction of a conditional π-phase gate. This difficulty can be avoided by performing a measurement after each primitive conditional φ_{NL}-phase gate that projects onto the principal-mode subspace, exploiting the quantum Zeno effect as an error-preventing mechanism [19–21]. For a particular choice of principal modes, we suggest one way that such a measurement could be realized.

We derive these results using a single $\vee$-type atom placed within a one-sided cavity as a microscopic model for XPM. While the nonlinearities present in a $\vee$ atom are not as strong as those in, for example, the giant Kerr effect [22,23], the $\vee$ system is simple enough that it yields readily to an analysis in terms of quantum fields. After solving for the evolution of our system in the one- and two-photon subspaces, we investigate fidelity and cascadability. It turns out that while cascading small phase shifts with projective measurements interleaved can produce a high-fidelity gate in principle, the number of cascades needed is impractically large when the $\vee$ system's weak nonlinearity is used to provide XPM. Nevertheless, the

idea of cascading through principal-mode projection is of potential use to overcome fidelity-degrading noise for a wide variety of nonlinear optical primitive gates.

II. THE FIELDS AND THEIR INTERACTION

In this section, we describe our encoding of qubit states in one-dimensional quantum fields, then consider how these fields evolve when interacting with an optical cavity containing an atomic ∨ system. Following the approach used in [7,24,25], this is described by a Hamiltonian $\mathcal{H}_{\text{NL}}$ for the fields + cavity + atom system. The Hamiltonian-based approach we use is essentially the basis for an alternative description in terms of the input-output formalism [26].

The atomic system mediates an XPM-like interaction that is a central component in the conditional phase gates discussed later. Determining the nonlinear phase shift and error induced by the atomic interaction will be of the utmost importance in evaluating these gates. To this end, one- and two-photon propagators for this system [24] are introduced.

A. Qubit encoding

In our gate, qubit states are encoded using two quasi-monochromatic, positive-frequency, photon units optical fields $h_z(\tau)$ and $v_z(\tau)$ [27] (for convenience, $\tau \equiv ct$ is used to measure time). We take $+z$ as the propagation direction and ignore the transverse character of these fields throughout. The horizontally polarized field $h_z(\tau)$ and the vertically polarized field $v_z(\tau)$ are independent and have a nontrivial commutator, $[h_z(\tau), h_{z'}(\tau)^{\dagger}] = [v_z(\tau), v_{z'}(\tau)^{\dagger}] = \delta(z - z')$.

Logical qubit states are encoded as excitations of two *principal modes* h and v, defined by

$$h^{\dagger} \equiv \int dz \, \psi(z) h_z^{\dagger}, \quad v^{\dagger} \equiv \int dz \, \psi(z) v_z^{\dagger}, \qquad (1)$$

where operators without explicit time dependence are in the Schrödinger picture. With the normalization $\int dz |\psi(z)|^2 = 1$, $h^{\dagger}$ and $v^{\dagger}$ are interpreted, respectively, as creating horizontally and vertically polarized photons with wave function $\psi(z)$. We refer to all modes orthogonal to h and v as *auxiliary*, or *bath*, modes and assume that the auxiliary modes are initially unexcited. In this case, the correspondence between logical qubit states and field states reads

$$|00\rangle_{\text{L}} \quad \leftrightarrow \quad |\text{vac}\rangle, \qquad (2a)$$

$$|01\rangle_{\text{L}} \quad \leftrightarrow \quad |H\rangle \equiv h^{\dagger}|\text{vac}\rangle, \qquad (2b)$$

$$|10\rangle_{\text{L}} \quad \leftrightarrow \quad |V\rangle \equiv v^{\dagger}|\text{vac}\rangle, \qquad (2c)$$

$$|11\rangle_{\text{L}} \quad \leftrightarrow \quad |HV\rangle \equiv v^{\dagger}h^{\dagger}|\text{vac}\rangle, \qquad (2d)$$

where $|\text{vac}\rangle$ is the multimode vacuum. Equation (2) could describe either a dual-rail or polarization encoding, where fields not participating in our gate have been dropped for convenience.

B. Qubit evolution and interaction Hamiltonian

At the input to our gate, the fields are prepared in some superposition $|\psi_{\text{in}}\rangle$ of the basis states in Eq. (2). This state is localized in a noninteracting input region [Fig. 1(a)]. It then propagates in the $+z$ direction toward a region where both
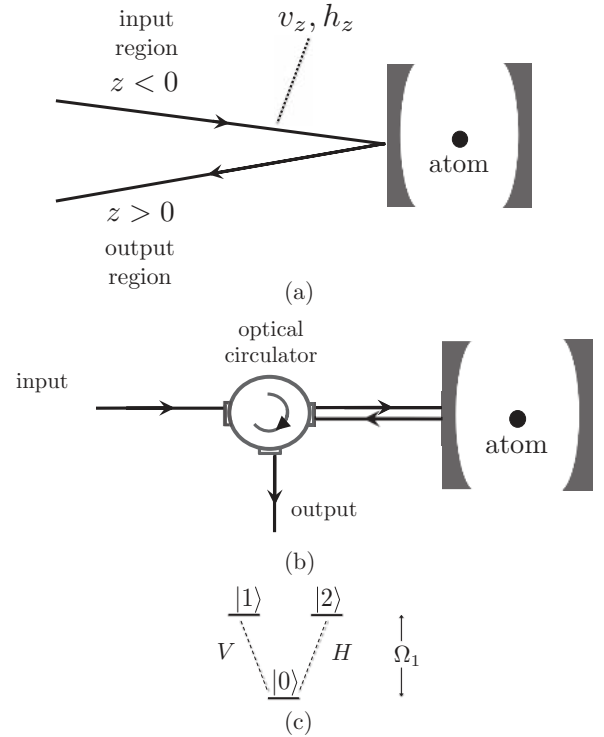

FIG. 1. (a) The external fields $v_z(\tau)$ and $h_z(\tau)$ interact with an atom placed within a one-sided cavity at position $z = 0$. (b) An optical circulator could be used to separate input and output fields in practice. (c) Three-level atom used as an XPM medium. Vertical light (V) drives the $0 \leftrightarrow 1$ transition, while horizontal light (H) drives the $0 \leftrightarrow 2$ transition. In the lossy-cavity regime, $\gamma_{\text{3D}} \ll g \ll \kappa$, the cavity fields can be adiabatically eliminated, yielding an effective coupling directly between the external fields and the ∨ system at strengths $\Gamma_{H(V)} = 4g_{H(V)}^2 / \kappa_{H(V)}$.

fields interact, evolving under a nonlinear total Hamiltonian $\mathcal{H}_{\text{NL}}$ which couples these fields to a three-level atomic ∨ system. (Here "nonlinear" means that the total Hamiltonian $\mathcal{H}_{\text{NL}}$ generates nonlinear Heisenberg equations of motion, which is a necessary condition for $\mathcal{H}_{\text{NL}}$ to effect a two-qubit gate that does not factorize into a product of one-qubit gates.) Much later, the atom has returned to its ground state and the photonic qubits are in a state $|\psi_1\rangle$, which is localized in a noninteracting output region. Working in an interaction picture with respect to the free-field Hamiltonian $\mathcal{H}_{\text{fields}}$, the scattering matrix connects the states $|\psi_{\text{in}}\rangle$ and $|\psi_1\rangle$:

$$|\psi_1\rangle = \mathcal{S}_{\text{NL}}|\psi_{\text{in}}\rangle, \quad \mathcal{S}_{\text{NL}} \equiv \lim_{\tau \to \infty} e^{i\mathcal{H}_{\text{fields}}\tau/\hbar c} e^{-i\mathcal{H}_{\text{NL}}\tau/\hbar c}. \qquad (3)$$

In interacting with the atom, a single horizontally polarized (vertically polarized) photon acquires a phase shift φ_H (φ_V), and may undergo some amount of pulse deformation. When both a horizontal and a vertical photon are incident upon the atom at the same time, however, the presence of the horizontal photon frustrates the interaction of the vertical photon with the atom, and vice versa, i.e., the atom cannot absorb both photons simultaneously. As a result, the pair of photons picks up an extra phase shift φ_{NL}. In this way, the ∨ system models a Kerr medium and can be used to construct conditional phase gates.

To describe this interaction, we use the same Hamiltonian $\mathcal{H}_{\text{NL}}$ as in [24]: both fields h_z and v_z couple to a one-sided

cavity containing an atomic $\vee$ system. For $z < 0$, these fields are interpreted as propagating toward the cavity, while for $z > 0$, they are interpreted as propagating away from the cavity [Fig. 1(a)]. As shown in Fig. 1(b), an optical circulator could be used in practice to achieve this separation of input and output fields. Figure 1(c) shows the $\vee$ system's level structure. All cavity modes are ignored, except a horizontally polarized mode a_H and a vertically polarized mode a_V, both of which are resonant with the atomic transitions at frequency Ω_1. The total Hamiltonian $\mathcal{H}_{\mathrm{NL}} = \mathcal{H}_0 + \mathcal{H}_{\text{fields-cav}} + \mathcal{H}_{\text{cav-atom}}$ is the sum of a noninteracting Hamiltonian $\mathcal{H}_0$ and two interaction pieces. In terms of k-space field operators $\widetilde{v}_k \equiv \int dz v_z e^{-ikz}$ and $\widetilde{h}_k \equiv \int dz h_z e^{-ikz}$, which annihilate photons with definite frequency, the noninteracting Hamiltonian $\mathcal{H}_0$ is

$$\mathcal{H}_0 = \mathcal{H}_{\text{fields}} + \mathcal{H}_{\text{cav}} + \mathcal{H}_{\text{atom}}, \tag{4a}$$

$$\mathcal{H}_{\text{fields}} = \int \frac{dk}{2\pi} \hbar \omega_k (\widetilde{h}_k^\dagger \widetilde{h}_k + \widetilde{v}_k^\dagger \widetilde{v}_k), \tag{4b}$$

$$\mathcal{H}_{\text{cav}} = \hbar \Omega_1 c (a_V^\dagger a_V + a_H^\dagger a_H), \tag{4c}$$

$$\mathcal{H}_{\text{atom}} = \hbar \Omega_1 c (\sigma_{11} + \sigma_{22}), \tag{4d}$$

wherein $\sigma_{mn} \equiv |m\rangle\langle n|$ and $\omega_k = ck$ [28]. Under $\mathcal{H}_0$, the Heisenberg-picture field operators propagate towards $+\infty$, e.g., $e^{-i\mathcal{H}_0\tau/\hbar c} h_z e^{i\mathcal{H}_0\tau/\hbar c} = h_{z-\tau}$.

The interactions between the cavity, free-field, and atom are taken within the rotating wave approximation, so that the total Hamiltonian $\mathcal{H}_{\mathrm{NL}}$ is

$$\mathcal{H}_{\mathrm{NL}} = \mathcal{H}_0 + \mathcal{H}_{\text{fields-cav}} + \mathcal{H}_{\text{cav-atom}}, \tag{5a}$$

$$\mathcal{H}_{\text{fields-cav}} = i\hbar c \kappa_V^{1/2} (v_0 a_V^\dagger - v_0^\dagger a_V)$$
$$+ i\hbar c \kappa_H^{1/2} (h_0 a_H^\dagger - h_0^\dagger a_H), \tag{5b}$$

$$\mathcal{H}_{\text{cav-atom}} = i\hbar c g_V (a_V \sigma_{10} - a_V^\dagger \sigma_{01})$$
$$+ i\hbar c g_H (a_H \sigma_{20} - a_H^\dagger \sigma_{02}). \tag{5c}$$

We have taken $z = 0$ as the cavity's position.

As in [24], we consider the lossy-cavity regime in which the cavity decay rates κ, cavity-atom couplings g, and rate γ_{3D} of spontaneous emission into free space satisfy $\kappa \gg g \gg \gamma_{3D}$. In this regime, cavity decay dominates spontaneous emission, and cavity operators can be adiabatically eliminated in favor of the external field [24,29], i.e., in the lossy-cavity regime, the atom couples directly to the one-dimensional input and output fields. The dynamics of the atom+external field system are then identical (up to an inconsequential phase shift resulting from reflection off the one-sided cavity's perfect mirror) to those generated by an effective Hamiltonian $\mathcal{H}'_{\mathrm{NL}}$ in which the fields are directly coupled to the atom,

$$\mathcal{H}'_{\mathrm{NL}} = \mathcal{H}_0 + i\hbar c \Gamma_H^{1/2} (v_0 \sigma_{10} - v_0^\dagger \sigma_{01})$$
$$+ i\hbar c \Gamma_V^{1/2} (h_0 \sigma_{20} - h_0^\dagger \sigma_{02}), \tag{6}$$

where the effective coupling is $\Gamma_{H(V)} = 4g_{H(V)}^2 / \kappa_{H(V)}$. In this paper, dynamics are derived exclusively from the effective Hamiltonian $\mathcal{H}'_{\mathrm{NL}}$. To ensure that the gate treats both qubits symmetrically, we will later set $\Gamma_H = \Gamma_V$, but temporarily retain subscripts for pedagogical clarity.

C. Evolution of one- and two-photon states

To determine how the one- and two-photon states in Eq. (2) that encode the computational basis evolve under the scattering matrix $\mathcal{S}_{\mathrm{NL}}$, it suffices to know the one- and two-photon propagators (the vacuum state evolves trivially). Labeling states $|\text{atom; field}\rangle$, these are

$$G_H(x,y) \equiv \langle 0; \text{vac}| h_x \mathcal{S}_{\mathrm{NL}} h_y^\dagger |0; \text{vac}\rangle, \tag{7a}$$

$$G_V(x,y) \equiv \langle 0; \text{vac}| v_x \mathcal{S}_{\mathrm{NL}} v_y^\dagger |0; \text{vac}\rangle, \tag{7b}$$

$$G_{HV}(x_H, x_V, y_H, y_V) \equiv \langle 0; \text{vac}| h_{x_H} v_{x_V} \mathcal{S}_{\mathrm{NL}} h_{y_H}^\dagger v_{y_V}^\dagger |0; \text{vac}\rangle. \tag{7c}$$

The time-dependent propagators—matrix elements of $e^{-i\mathcal{H}'_{\mathrm{NL}}\tau/\hbar c}$ instead of $\mathcal{S}_{\mathrm{NL}}$—are given in [24].

The single-photon propagator $G_H(x,y)$ gives the long-time, interaction-picture amplitude for a photon initially at position y to propagate to position x. We will always assume that $y < 0$ so that every photon can interact with the atom, located at the origin. In this case,

$$G_H(x,y) = \delta(x - y) - \Gamma_H^{1/2} R_H(y - x), \tag{8}$$

where

$$\Gamma_H^{-1/2} R_H(\tau) \equiv \theta(\tau)\langle 1; \text{vac}| e^{-i\mathcal{H}'_{\mathrm{NL}}\tau/\hbar c} |1; \text{vac}\rangle$$
$$= \theta(\tau) e^{-(i\Omega_1 + \Gamma_H/2)\tau} \tag{9}$$

is the amplitude for the atom, excited by a horizontally polarized impulse at time zero, to still be excited at a time τ later. Here $\theta(\tau)$ is the Heaviside step function, equal to 1 for $\tau > 0$ and 0 for $\tau < 0$. The Fourier-space propagator $\widetilde{G}_H(k,q) \equiv \langle 0; \text{vac}| \widetilde{h}_k \mathcal{S} \widetilde{h}_q^\dagger |0; \text{vac}\rangle$ is also useful. Using Eq. (8), it is

$$\widetilde{G}_H(k,q) = \int dx dy\, G_H(x,y) e^{iqy - ikx}$$
$$= 2\pi \delta(k - q) \frac{k - \Omega_1 - i\Gamma_H/2}{k - \Omega_1 + i\Gamma_H/2}. \tag{10}$$

Analogous results hold for $G_V(x,y)$.

If the atomic system were linear, it could absorb multiple photons before emitting any. In this case, the two-photon propagator $G_{HV}(x_H, x_V, y_H, y_V)$ would just be a product of single-photon propagators. Instead, it is

$$G_{HV}(x_H, x_V, y_H, y_V) = G_H(x_H, y_H) G_V(x_V, y_V) - \Gamma_H^{1/2} \Gamma_V^{1/2}$$
$$\times R_H(y_H - x_H) R_V(y_V - x_V)$$
$$\times \theta(\min[y_H, y_V] - \max[x_H, x_V]). \tag{11}$$

Here the second piece removes from $G_H(x_H, y_H) G_V(x_V, y_V)$ exactly those terms that correspond to two absorptions before any emissions. This causes two-photon output states to be antibunched.

The corresponding two-photon Fourier-space propagator is

$$\widetilde{G}_{HV}(k_H, k_V, q_H, q_V) = \widetilde{G}_H(k_H, q_H) \widetilde{G}_V(k_V, q_V)$$
$$+ i\Gamma_H \Gamma_V (2\pi) \delta(k_H + k_V - q_H - q_V)$$
$$\times \frac{1}{\widetilde{\delta}_{k_H}^{(H)}} \frac{1}{\widetilde{\delta}_{k_V}^{(V)}} \left(\frac{1}{\widetilde{\delta}_{q_H}^{(H)}} + \frac{1}{\widetilde{\delta}_{q_V}^{(V)}} \right), \tag{12}$$

wherein $\widetilde{\delta}_k^{(H/V)} \equiv k - \Omega_0 + i\Gamma_{H/V}/2$. The Fourier-space propagators $\widetilde{G}_H, \widetilde{G}_V$, and $\widetilde{G}_{HV}$ enable the gate fidelity calculations reported in Sec. III C.

III. A PRIMITIVE CONDITIONAL PHASE GATE

In this section, we describe a conditional phase gate based on the interaction $\mathcal{S}_{\text{NL}}$ described above. We first discuss how the unnecessary and undesirable linear evolution can be removed. We then consider the fidelity of this primitive (noncascaded) gate with an ideal conditional phase gate.

A. Removing linear evolution

In interacting with the atomic $\vee$ system, both the one- and two-photon states that encode the computational basis [Eq. (2)] evolve nontrivially:

$$|H\rangle \xrightarrow{\mathcal{S}_{\text{NL}}} (1 - |\varepsilon_H|^2)^{1/2} e^{i\varphi_H} |H\rangle + \varepsilon_H |e_H\rangle, \tag{13a}$$

$$|V\rangle \xrightarrow{\mathcal{S}_{\text{NL}}} (1 - |\varepsilon_V|^2)^{1/2} e^{i\varphi_V} |V\rangle + \varepsilon_V |e_V\rangle, \tag{13b}$$

$$|HV\rangle \xrightarrow{\mathcal{S}_{\text{NL}}} (1 - |\varepsilon_{HV}|^2)^{1/2} e^{i(\varphi_H + \varphi_V + \varphi_{\text{NL}})} |HV\rangle + \varepsilon_{HV} |e_{HV}\rangle. \tag{13c}$$

Here all kets are normalized, $\{\varphi_H, \varphi_V\}$ are the single-photon (linear) phase shifts, and the various ε terms represent errors that occur because of photons evolving out of the principal modes.

The linear phase shifts $\{\varphi_H, \varphi_V\}$ are not only irrelevant to the construction of conditional logic gates, but come also with some amount of fidelity-degrading evolution out of the principal-mode subspace. In order to build high-fidelity gates, it would be useful to remove completely the linear evolution that causes these effects. Removing linear evolution is also theoretically appealing because it allows one to study the fundamental limitations of the $\vee$ system's capacity for quantum XPM.

Formally, linear evolution is removed by evolving backward in time under a linearized Hamiltonian $H_{\text{L}}(\Omega_1)$ in which the atomic lowering operators σ_{01} and σ_{02} are replaced by independent harmonic-oscillator annihilation operators b_V and b_H [cf. Eq. (6)],

$$\begin{aligned}
\mathcal{H}_{\text{L}}(\Omega_1) = \mathcal{H}_{\text{fields}} &+ \hbar c \Omega_1 (b_V^\dagger b_V + b_H^\dagger b_H) \\
&+ i\hbar c \Gamma_H^{1/2} (v_0 b_V^\dagger - v_0^\dagger b_V) \\
&+ i\hbar c \Gamma_V^{1/2} (h_0 b_H^\dagger - h_0^\dagger b_H).
\end{aligned} \tag{14}$$

This Hamiltonian, which we have explicitly parametrized by the cavity frequency Ω_1 for later convenience, is linear in the sense that the equations of motion which it generates for the field operators $h_z(\tau)$ and $v_z(\tau)$ are linear differential equations. Application of the corresponding inverse scattering matrix $\mathcal{S}_{\text{L}}^\dagger(\Omega_1) \equiv \lim_{\tau \to \infty} e^{-i\mathcal{H}_{\text{fields}}(\Omega_1)\tau/\hbar c} e^{+i\mathcal{H}_{\text{L}}(\Omega_1)\tau/\hbar c}$ then removes linear evolution from $\mathcal{S}_{\text{NL}}$.

This useful form of error correction can, in principle, be implemented using linear optics. Figure 2(a) shows an optical circuit that removes linear evolution from input photons with center wave number k_0 by simulating time-reversed evolution under Eq. (14). The idea is to run the photons through $\mathcal{H}_{\text{L}}$ backwards: first, the baseband modulation of the input photon
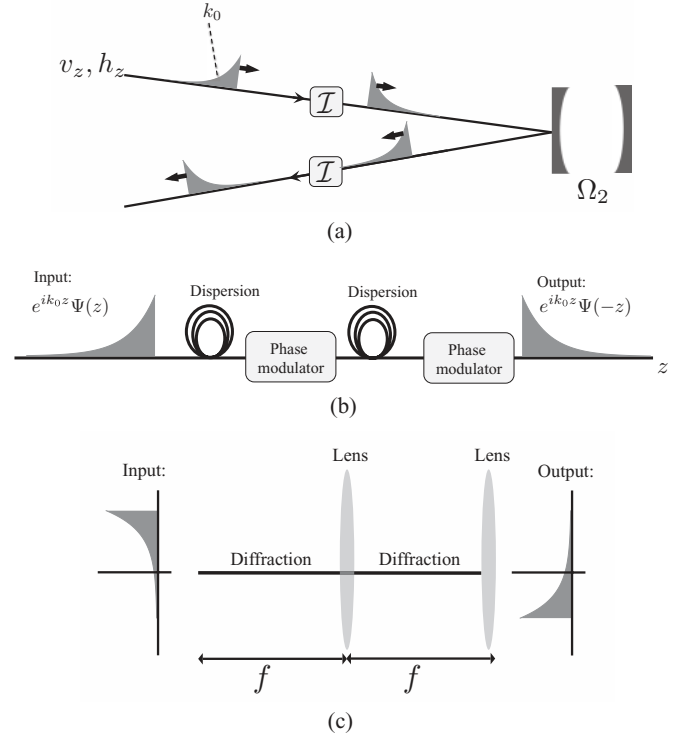

FIG. 2. (a) Optical circuit to simulate time-reversed evolution under Eq. (14). The cavity frequency Ω_2 is chosen so that $k_0 - \Omega_1 = -(k_0 - \Omega_2)$. (b) Temporal imaging system to realize inversion $\mathcal{I}$ about center frequency k_0, using two dispersive delay lines and two quadratic phase modulators. (c) The analogous spatial imaging system using free-space diffraction and thin lenses.

pulses is inverted ($\mathcal{I}$); the pulses then interact with empty one-sided cavities; finally, the baseband modulation is reinverted.

Real-space inversion of an optical pulse's baseband modulation corresponds to inversion about its center wave number k_0 in Fourier space. This transformation,

$$\mathcal{I}^\dagger \widetilde{h}_k \mathcal{I} = \widetilde{h}_{2k_0 - k}, \tag{15}$$

can be achieved using temporal imaging [30–33]. Temporal imaging is the longitudinal analog of traditional spatial imaging: in spatial imaging, a beam's transverse profile is manipulated using free-space diffraction and thin lenses; in temporal imaging, the longitudinal (temporal) profile is manipulated using dispersive delay lines and quadratic phase modulation. Figure 2(b) shows a temporal imaging system for baseband modulation inversion, while Fig. 2(c) shows its spatial analog.

While this method has not, to our knowledge, been used to demonstrate pulse inversion with quantum light, we see no fundamental physical principle preventing its implementation. Because the scheme to implement $\mathcal{I}$ shown in Fig. 2(b) involves only passive linear field transformations (dispersion and phase modulation), it behaves identically with respect to classical fields and few-photon pulses.

After inverting the optical pulses, the fields in Fig. 2(a) evolve forward in time under the linearized Hamiltonian $\mathcal{H}_{\text{L}}(\Omega_2)$ with cavity frequency Ω_2. This corresponds to applying $\mathcal{S}_{\text{L}}(\Omega_2)$ on the field operators. Because the equations of motion generated by $\mathcal{H}_{\text{L}}(\Omega_2)$ are linear, the mapping of the

field operators under $\mathcal{S}_{\mathrm{L}}(\Omega_2)$ is analogous to the mapping of single-photon packets under $\mathcal{S}_{\mathrm{NL}}$ [Eq. (10)],

$$\mathcal{S}_{\mathrm{L}}^{\dagger}(\Omega_2)\widetilde{h}_k\mathcal{S}_{\mathrm{L}}(\Omega_2) = \widetilde{h}_k\frac{k - (\Omega_2 + i\Gamma_H/2)}{k - (\Omega_2 - i\Gamma_H/2)}, \qquad (16)$$

and similarly for v_k. By picking the pulse center wave number k_0, atomic resonance Ω_1, and cavity resonance Ω_2, such that photon-atom and photon-cavity detunings are equal and opposite, viz., $k_0 - \Omega_1 = -(k_0 - \Omega_2)$, the combined effect of pulse inversion, followed by evolution under $\mathcal{H}_{\mathrm{L}}(\Omega_2)$, followed by pulse inversion, yields time-reversed evolution under $\mathcal{H}_{\mathrm{L}}(\Omega_1)$:

$$\mathcal{I}\mathcal{S}_{\mathrm{L}}(\Omega_2)\mathcal{I} = \mathcal{S}_{\mathrm{L}}^{\dagger}(\Omega_1). \qquad (17)$$

In this way, the linear portion of $\mathcal{S}_{\mathrm{NL}}$ can be undone.

B. The primitive gate

The combined effect of nonlinear interaction with the $\vee$ system and removal of linear evolution is evolution under $\mathcal{S}_{\mathrm{L}}^{\dagger}\mathcal{S}_{\mathrm{NL}}$:

$$|\mathrm{vac}\rangle \xrightarrow{\mathcal{S}_{\mathrm{L}}^{\dagger}\mathcal{S}_{\mathrm{NL}}} |\mathrm{vac}\rangle, \qquad (18a)$$

$$|H\rangle \xrightarrow{\mathcal{S}_{\mathrm{L}}^{\dagger}\mathcal{S}_{\mathrm{NL}}} |H\rangle, \qquad (18b)$$

$$|V\rangle \xrightarrow{\mathcal{S}_{\mathrm{L}}^{\dagger}\mathcal{S}_{\mathrm{NL}}} |V\rangle, \qquad (18c)$$

$$|HV\rangle \xrightarrow{\mathcal{S}_{\mathrm{L}}^{\dagger}\mathcal{S}_{\mathrm{NL}}} (1 - |\varepsilon|^2)e^{i\varphi_{\mathrm{NL}}}|HV\rangle + \varepsilon|e\rangle. \qquad (18d)$$

Here $|e\rangle$ is a two-photon state whose presence reflects errors intrinsic to the nonlinear evolution only. We refer to the Eq. (18) transformation as our *primitive* conditional φ_{NL}-phase gate; this gate is primitive in the sense that it is not built by cascading simpler logic gates.

It is convenient to describe the primitive gate as transformation on the logical subspace $\{|\mathrm{vac}\rangle, |H\rangle, |V\rangle, |HV\rangle\}$ alone. For nonzero errors ε, the mapping given by Eq. (18) between input and output field states is not unitary when restricted to this subspace because of pulse deformation and undesirable entanglement generated between continuous degrees of freedom (e.g., photon momentum). When restricted to the logical subspace, Eq. (18) corresponds to a trace-preserving quantum operation $\mathcal{E}_{\mathrm{prim}}$:

$$\mathcal{E}_{\mathrm{prim}}(\rho) = U_{\varphi_{\mathrm{NL}}}(E_1\rho E_1^{\dagger} + E_2\rho E_2^{\dagger})U_{\varphi_{\mathrm{NL}}}^{\dagger}. \qquad (19)$$

Here ρ is a two-qubit density matrix, U_{φ} is the ideal conditional φ-phase gate, and the operation elements $\{E_1, E_2\}$ represent pure amplitude damping of the two-photon state $|HV\rangle$ out of the logical subspace. In the usual basis,

$$U_{\varphi} = \begin{bmatrix} 1 & 0 & 0 & 0 \\ 0 & 1 & 0 & 0 \\ 0 & 0 & 1 & 0 \\ 0 & 0 & 0 & e^{i\varphi} \end{bmatrix}, \qquad (20a)$$

$$E_1 = \begin{bmatrix} 1 & 0 & 0 & 0 \\ 0 & 1 & 0 & 0 \\ 0 & 0 & 1 & 0 \\ 0 & 0 & 0 & (1-|\varepsilon|^2)^{1/2} \end{bmatrix}, \qquad (20b)$$

$$E_2 = \begin{bmatrix} 0 & 0 & 0 & \varepsilon \\ 0 & 0 & 0 & 0 \\ 0 & 0 & 0 & 0 \\ 0 & 0 & 0 & 0 \end{bmatrix}. \qquad (20c)$$

This operator-sum representation of the primitive gate is useful in determining its fidelity with an ideal conditional phase gate.

C. Fidelity of a single gate

The *fidelity* of two states is a measure of how close they are to one another, increasing from 0 (orthogonal states) to 1 (identical states). The fidelity of a pure state ψ with a mixed state ρ may be defined as their overlap, $F(|\psi\rangle, \rho) = \langle\psi|\rho|\psi\rangle$. *Gate fidelity* extends this idea from states to logical operations on qubits. The (minimum) gate fidelity of a quantum operation $\mathcal{E}$ with a unitary gate U that $\mathcal{E}$ approximates is the fidelity of $\mathcal{E}$'s output with the target output, minimized over pure state inputs [34],

$$F(\mathcal{E}, U) = \min_{|\psi\rangle}\langle\psi|U^{\dagger}\mathcal{E}(|\psi\rangle\langle\psi|)U|\psi\rangle. \qquad (21)$$

The infidelity $1 - F(\mathcal{E}, U)$ is the (maximum) probability that the $\mathcal{E}$ fails to effect the desired transformation U.

The fidelity of our gate $\mathcal{E}_{\mathrm{prim}}$ with the ideal conditional phase gate $U_{\varphi_{\mathrm{NL}}}$ is

$$\begin{aligned}F(\mathcal{E}_{\mathrm{prim}}, U_{\varphi_{\mathrm{NL}}}) &\equiv \min_{|\psi\rangle}\langle\psi|U_{\varphi_{\mathrm{NL}}}^{\dagger}\mathcal{E}_{\mathrm{prim}}(|\psi\rangle\langle\psi|)U_{\varphi_{\mathrm{NL}}}|\psi\rangle \\ &= \min_{|\psi\rangle}[|\langle\psi|E_1|\psi\rangle|^2 + |\langle\psi|E_2|\psi\rangle|^2] \\ &= 1 - |\varepsilon|^2. \qquad (22)\end{aligned}$$

Here the minimizing state is $|11\rangle_{\mathrm{L}} = |HV\rangle$.

We now consider the relationship between the fidelity $F(\mathcal{E}_{\mathrm{prim}}, U_{\varphi_{\mathrm{NL}}})$ and the nonlinear phase shift when the real-space principal-mode wave function $\psi(z)$ in Eq. (23) is a rising exponential with center wave number k_0 and width γ,

$$\psi(z) \equiv e^{ik_0 z}\Psi(z), \quad \Psi(z) = \theta(-z)\gamma^{1/2}e^{-\gamma|z|/2}. \qquad (23)$$

This particular principal-mode wave function is chosen because, as demonstrated in the next section, it is possible to make a projective measurement that distinguishes excitations of this principal mode from all other modes by exploiting the fact that photons with exponential wave functions are created when excited atoms decay. This fact can also be used to generate such photons and is the basis of several microwave-frequency single-photon sources that use artificial atoms coupled to superconducting resonators [35–37].

Henceforth we specialize to the case in which $\Gamma_H = \Gamma_V \equiv \Gamma$ in order that the qubits are treated symmetrically.

Large phase shifts. If the fidelity $F(\mathcal{E}_{\mathrm{prim}}, U_{\varphi_{\mathrm{NL}}})$ and phase shift φ_{NL} could both be large simultaneously, then the primitive gate would be an effective conditional phase gate.

It is only when the atomic linewidth Γ is comparable in size to the pulse bandwidth γ that a large nonlinear phase shift is possible. If $\gamma \gg \Gamma$, then the pulse is too broadband to interact significantly with the atom, while if $\gamma \ll \Gamma$, then one sees from Eq. (11) that the range Γ^{-1} of the nonlinear piece of the two-photon propagator is negligible in comparison to the pulse length γ^{-1}.
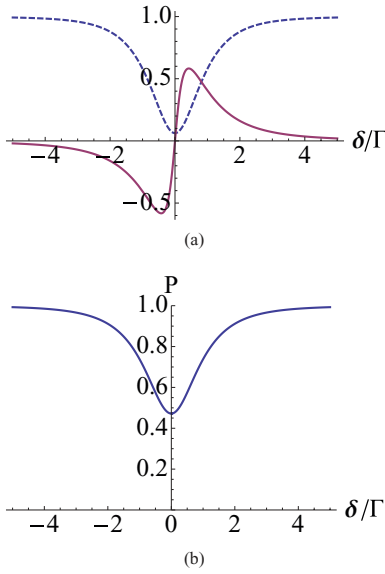
FIG. 3. (Color online) (a) Comparison of the fidelity (dashed line) and nonlinear phase (solid line) when $\gamma = \Gamma$ as a function of the detuning δ. (b) Purity $P = \mathrm{tr}\,\rho_H'^2$ of the horizontal photon's output density matrix when the input state is $|HV\rangle$ as a function of δ when $\gamma = \Gamma$.

Figure 3(a) shows the fidelity and nonlinear phase shift as functions of the detuning $\delta \equiv k_0 - \Omega_1$ in the particular case $\gamma = \Gamma$. The phase shift $\varphi_{\mathrm{NL}}(\delta)$ has the form of a dispersion curve, while the infidelity $1 - F$ mimics an absorption curve. The figure shows that while large nonlinear phase shifts are possible for nearly resonant pulses, the fidelity is unacceptably low in these cases—a conclusion similar to those drawn in [8,10].

A large contribution to this fidelity degradation is the entanglement generated between the position (or momentum) coordinates of the horizontally and vertically polarized photons. This entanglement reflects antibunching in the two-photon output wave function and is characterized by a subunity purity $P \equiv \mathrm{tr}\,\rho_H'^2$ of the horizontal photon's output density matrix $\rho_H' \equiv \mathrm{tr}_V\,\mathcal{E}(|HV\rangle\langle HV|)$ [Fig. 3(b)].

Small phase shifts. While large phase shifts are accompanied by large errors, it is possible to achieve small phase shifts with a much smaller error: $|\varepsilon|^2 \ll \varphi_{\mathrm{NL}} \ll 1$. When the phase shift and error are small, it is convenient to write

$$\langle HV | \mathcal{S}_{\mathrm{L}}^{\dagger} \mathcal{S}_{\mathrm{NL}} | HV \rangle = 1 + i\zeta, \tag{24}$$

so that to lowest order in ζ the nonlinear phase shift is $\varphi_{\mathrm{NL}} = \mathrm{Re}[\zeta]$ and error probability $1 - F$ is $|\varepsilon|^2 = 2\mathrm{Im}[\zeta]$.

Particularly simple expressions for the phase shift and error are obtained when the pulse bandwidth is much less than the atomic linewidth, $\gamma \ll \Gamma$. Because the photon wave function $\psi(z)$ has length $\sim \gamma^{-1}$ and is normalized to unity, this can be considered a sort of weak-excitation regime. In this case, ζ is readily calculated from the Fourier-space propagators, given by Eqs. (10) and (12). One finds that in this case, dependences of φ_{NL} and $|\varepsilon|^2$ on the detuning are again those of dispersion

and absorption curves,

$$\varphi_{\mathrm{NL}} = \frac{\gamma \Gamma^2 \delta}{[\delta^2 + (\Gamma/2)^2]^2}, \tag{25a}$$

$$|\varepsilon|^2 = \frac{\Gamma}{\delta}\varphi_{\mathrm{NL}}, \tag{25b}$$

to lowest nonvanishing order in γ / Γ.

From Eq. (25), it is clear that when $\gamma \ll \Gamma \ll \delta$, the nonlinear phase shift, while very small, is large in comparison to the error probability: $|\varepsilon|^2 \ll \varphi_{\mathrm{NL}}$. Actually, the relation $|\varepsilon|^2 \ll \varphi_{\mathrm{NL}}$ can be achieved without requiring that $\gamma \ll \Gamma$: it is enough for the photons to be far detuned. When $\Gamma, \gamma \ll \delta$, we have

$$\varphi_{\mathrm{NL}} = \mathrm{Re}[\zeta] = \frac{\gamma \Gamma^2}{\delta^3}\left(\frac{1 + 5\frac{\gamma}{\Gamma}}{1 + \frac{\gamma}{\Gamma}}\right), \tag{26a}$$

$$|\varepsilon|^2 = 2\mathrm{Im}[\zeta] = \frac{\Gamma}{\delta}\left(\frac{1 + 10\frac{\gamma}{\Gamma} + \frac{\gamma^2}{\Gamma^2}}{1 + 5\frac{\gamma}{\Gamma}}\right)\varphi_{\mathrm{NL}}, \tag{26b}$$

to lowest order in $\max[\gamma, \Gamma]/\delta$. Again, the nonlinear phase shift, though small, is much larger than the infidelity $|\varepsilon|^2$. In this sense, our primitive conditional phase gate can be considered high fidelity for small phase shifts.

IV. CASCADING SMALL PHASE SHIFTS

The error $|\varepsilon|^2$ in the primitive conditional phase gate discussed above is the probability that the gate causes the two-photon state $|HV\rangle$ to leak out of the principal-mode subspace. Because this error probability can be made much smaller than the phase shift in the far-detuned regime, the possibility of cascading $N = \pi/\varphi_{\mathrm{NL}}$ primitive gates to produce a high-fidelity conditional π-phase gate arises.

When the primitive gate $\mathcal{S}_{\mathrm{L}}^{\dagger}\mathcal{S}_{\mathrm{NL}}$ is cascaded N times, two sorts of errors can occur. With each application, the probability of photons leaking out of the principal-mode subspace increases; for small $|\varepsilon|^2$, these *leakage errors* grow as $N|\varepsilon|^2 = \pi|\varepsilon|^2/\varphi_{\mathrm{NL}} \ll 1$ and are not terribly problematic. However, amplitude that leaked from the principal-mode subspace in earlier applications of $\mathcal{S}_{\mathrm{L}}^{\dagger}\mathcal{S}_{\mathrm{NL}}$ can return in later applications with corrupted phase; these *coherent feedback errors* can grow as $N^2|\varepsilon|^2$, which is not small. Alternatively, this difficulty can be seen by noting that the primitive gate cascaded N times does *not* correspond to the quantum operation $\mathcal{E}_{\mathrm{prim}}$ cascaded N times. This is because the state of the auxiliary modes changes with each application of the $\mathcal{S}_{\mathrm{L}}^{\dagger}\mathcal{S}_{\mathrm{NL}}$.

A. A cascadable primitive gate

We propose to eliminate coherent feedback errors by measuring the number of photons present in the auxiliary modes after each application of the primitive gate. For the sake of the following analysis, the result of this measurement need not be considered, only that with probability of at least $1 - |\varepsilon|^2$ it projects the quantum state back onto the principal-mode subspace. For this reason, we call this measurement process *principal-mode projection* (PMP). Performing PMP after each application of the primitive gate is a sort of Zeno effect error correction that prevents amplitude from leaking out of the principal-mode subspace too quickly.
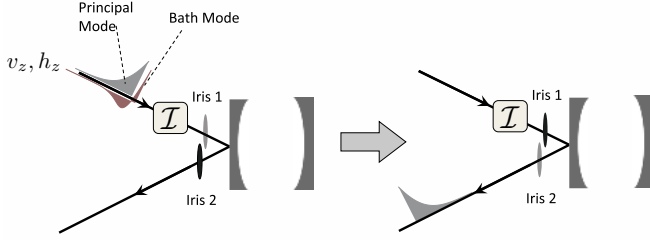
FIG. 4. (Color online) Schematic of a principal-mode projector for mode function given by Eq. (23). Initially, iris 1 is open, and photons from the principal mode are absorbed by the cavity after inversion. After principal-mode photons have been absorbed, iris 1 is shut and iris 2 is open, allowing cavity photons to be reemitted into the principal mode.

Crucially, the measurement used to implement PMP must be done in such a way that it is insensitive to the number of photons in the principal modes. If the principal-mode function $\psi(z)$ is chosen to be the one-sided exponential used above [Eq. (23)], then such a measurement can, in fact, be performed using empty optical cavities, the pulse inverter $\mathcal{I}$ introduced in Sec. III A, and irises.

The scheme, illustrated in Fig. 4 and analyzed in the Appendix, exploits the fact that (ignoring free-space evolution) a cavity with resonant wave number k_0 and decay rate γ preferentially emits photons with mode functions $e^{ik_0 z}\Psi(z)$ and preferentially absorbs from the inverted mode $e^{ik_0 z}\Psi(-z)$. This selectivity is used to load all principal-mode photons into optical cavities. That possibility is enabled by our gates being run on a clocked protocol; the known group velocity and principal-mode shape provide the necessary timing for the irises in Fig. 4. So, once the principal-mode photons have been loaded, iris 1 is closed, preventing non-principal-mode photons from entering the cavity, while iris 2 is opened, allowing the cavity photons to be emitted back into the principal modes. This setup could be modified to record the result of the PMP measurement, allowing for heralded operation and postselection. However, the point of the present analysis is to provide a design for a deterministic gate, and thus our process employs no postselection.

Figure 5 shows the entire process: interaction with the $\vee$ system ($\mathcal{S}_{NL}$), followed by removal of linear evolution ($\mathcal{S}_L^\dagger$), followed by PMP. (Note that the second and third pulse inverters cancel, and thus need not actually be implemented.) This gate, which we call the *cascadable primitive* gate, is
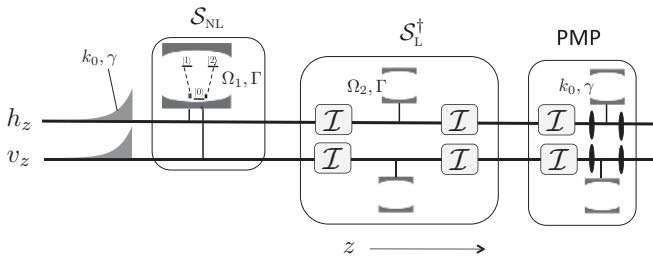

FIG. 5. The cascadable primitive gate. First, nonlinear evolution is provided by interaction with the atomic $\vee$ system. Linear evolution is then removed. Finally, principal-mode projection is performed.

most naturally represented by a non-trace-preserving quantum operation [34],

$$\mathcal{E}_{\text{c-prim}}(\rho) = U_{\varphi_{NL}} E_1 \rho E_1^\dagger U_{\varphi_{NL}}^\dagger, \qquad (27)$$

where $\text{tr}[\mathcal{E}_{\text{c-prim}}(\rho)]$ is the probability of success, i.e., that the output state has been collapsed into the principal-mode subspace.

B. Fidelity of the cascaded gate

Because of the PMP, the cascadable primitive gate can be cascaded $N = \pi/\varphi_{NL}$ times to produce a high-fidelity conditional π-phase gate. Without any postselection, the fidelity of this cascaded gate with the ideal conditional π-phase gate is the probability that PMP success occurs N times:

$$\begin{aligned} F(\mathcal{E}_{\text{c-prim}}^N, U_\pi) &= F(\mathcal{E}_{\text{c-prim}}, U_{\varphi_{NL}})^N \\ &= 1 - \pi \frac{\Gamma}{\delta}\left(\frac{1 + 10\frac{\gamma}{\Gamma} + \frac{\gamma^2}{\Gamma^2}}{1 + 5\frac{\gamma}{\Gamma}}\right), \qquad (28) \end{aligned}$$

to lowest nonvanishing order in $\max[\gamma, \Gamma]/\delta$. In the far-detuned regime $\gamma, \Gamma \ll \delta$, this fidelity can become quite large: cascading $\mathcal{E}_{\text{c-prim}}$ can yield a high-fidelity conditional π-phase gate.

As expected, because the $\vee$ system's nonlinearity is so weak, an unrealistic number of cascades N are required to produce a high-fidelity conditional π-phase gate. That impracticality is the price paid for having chosen a system whose simplicity admits to rigorous analysis.

For fixed N, Eq. (28) can be rewritten, after optimizing the ratio γ/Γ, as

$$F\left(\mathcal{E}_{\text{c-prim}}^N, U_\pi\right) \approx 1 - 4.82 \times N^{-1/3}. \qquad (29)$$

To achieve a fidelity greater than 95%, more than 10^6 cascades are required. A realization of our primitive gate using the 6.8 GHz microwave photons with exponential decay time $(\gamma c)^{-1} = 40$ ns generated in [36] and chirped delay-line-based temporal imaging as in [38,39] would take roughly 800 ns. The vast majority of this time is used loading photons into the PMP cavity. The 95%-fidelity conditional π-phase shift thus takes 0.8 s, which is prohibitively long.

The origin of this $N^{-1/3}$ scaling is the weak cross-phase shift, $\varphi_{NL} \propto \delta^{-3}$. If instead the phase shift and error were $\varphi_{NL} \propto \delta^{-m}$ and $|\varepsilon|^2 \propto \delta^{-n}$, respectively, the fidelity of the cascaded gate would be $F \sim 1 - N^{1-n/m}$. For example, $n = 2$ and $m = 1$ (as in the giant Kerr effect [22,23]) would lead to $F = 1 - 5 \times N^{-1}$ (assuming a prefactor similar to the $\vee$-system gate). In this case, 100 cascades would suffice for producing a 95%-fidelity conditional π-phase shift in about 40 μs.

Our cascadable primitive gate $\mathcal{E}_{\text{c-prim}}$ operates in the far-detuned regime and incorporates two error-correcting steps: the removal of linear evolution ($\mathcal{S}_L^\dagger$) and the PMP. Principal-mode projection is absolutely essential in making this gate cascadable. How important is removing the linear evolution? For the mode function used above, the linear errors $\{|\varepsilon_H|^2, |\varepsilon_V|^2\}$ must be removed. It turns out that because the Fourier-space mode function $\widetilde{\psi}(k) = i\gamma^{1/2}(k - k_0 + i\gamma/2)^{-1}$ falls off only as k^{-1}, linear errors are of the same order of magnitude as the nonlinear phase shift. However, for

more well-behaved Fourier-space mode functions (e.g., Gaussians $\widetilde{\psi}(k) \sim \exp\left[-(k-k_0)^2/4\gamma^2\right]$ and even Lorentzians $\widetilde{\psi}(k) \sim [(k-k_0)^2 + \gamma^2]^{-1}$), linear errors are of the same order as nonlinear errors. If PMPs could be constructed for these modes, the removal of linear evolution would not be essential.

V. CONCLUSIONS

Treating light as a multimode quantum field, we have described conditional phase gates in which photonic qubits interact with a three-level $\vee$ system. Although we have used the language of atomic and optical systems in our analysis, other implementations are possible. In the microwave, for example, the one-dimensional field of transmission-line waveguides have been coupled to artificial atoms [40,41].

In the regime of large nonlinear phase shifts, our primitive (noncascaded) gate has unacceptably low fidelity, as has been found for other gates relying on quantum cross-phase modulation [8–10]. We attribute much of this infidelity to undesirable entanglement generated by the local character of the nonlinear interaction between the horizontally and vertically polarized fields.

In contrast, the primitive gate can produce a small nonlinear phase shift with very high fidelity ($1 - F \ll \varphi_{\text{NL}}$) by operating in the far-detuned regime. However, one cannot straightforwardly cascade this high-fidelity, small conditional phase shift because of coherent feedback errors that grow as N^2.

We have shown that it is, in principle, possible to overcome the cascadability problem by making a projective measurement of the bath modes' photon number after each small conditional phase gate. With high probability, this measurement projects the field state back onto the information-carrying principal modes. This step—principal-mode projection—uses the quantum Zeno effect to prevent coherent feedback errors from occurring, making a cascadable primitive conditional phase gate.

We suggest that principal-mode projection could be a helpful subroutine in the future of photonic quantum information processing. While the $\vee$ system's weak cross-phase shift makes cascading our gate impractical [Eq. (29)], PMP together with stronger nonlinearities, e.g., the giant Kerr effect, could potentially realize a conditional π-phase gate whose fidelity scales more favorably with N. Moreover, for the often considered use of fiber XPM, PMP may provide a way to circumvent the phase-noise problem identified in [8,9]. While its utility in this regard can be evaluated theoretically, should that analysis be promising, a key challenge will be finding a practical PMP realization for fiber.

APPENDIX: PRINCIPAL-MODE PROJECTION WITH CAVITIES

In Sec. IV A, we outlined how principal-mode projection could be achieved for the one-sided exponential mode

$\psi(z) = \theta(-z)\gamma^{1/2}e^{(ik_0+\gamma/2)z}$ by exploiting the fact that cavities absorb and emit forward-decaying and backward-decaying exponential pulses. Here we give some mathematical details.

The PMP setup is shown in Fig. 4 and relies on a cavity whose resonant frequency ck_0 and decay rate γ are matched to the pulse shape $\psi(z)$. We assume the cavity is placed at position $z = L$. Ignoring the pulse inverter $\mathcal{I}$ for the moment, the interaction between the field v_z and cavity is described by a Hamiltonian

$$\mathcal{H} = \mathcal{H}_{\text{field}} + \hbar ck_0 b^\dagger b + i\hbar c\gamma^{1/2}(v_L b^\dagger - v_L^\dagger b), \quad \text{(A1a)}$$

$$\mathcal{H}_{\text{field}} = \int \frac{dk}{2\pi}\hbar ck\widetilde{v}_k^\dagger \widetilde{v}_k = -i\hbar c\int dz\, v_z^\dagger \partial_z v_z, \quad \text{(A1b)}$$

where b is the cavity lowering operator and $\widetilde{v}_k = \int dz\, v_z e^{-ikz}$, as above. Under this Hamiltonian, the Heisenberg equation of motion for $v_z(\tau)$ can be readily solved. For $\tau > 0$, the solution is $v_z(\tau) = v_{z-\tau} - \gamma^{1/2}\theta(z-L)\theta(\tau+L-z)b(\tau+L-z)$.

Initially, the cavity in Fig. 4 is empty and the field contains one photon in a mode $\phi(z)$ (assumed to be localized in the region $z < L$):

$$|\phi(0)\rangle = \int dz\,\phi(z)v_z^\dagger|0; \text{vac}\rangle. \quad \text{(A2)}$$

The amplitude for this photon to have been absorbed by the cavity at a time τ later is $s_V(\tau) = \langle 1; \text{vac}|e^{-i\mathcal{H}\tau/\hbar c}|\phi(0)\rangle$. By using Eq. (A2) to expand $|\phi(0)\rangle$ and using the Heisenberg equations of motion for $v_z(\tau)$ and $b(\tau)$, one can show that $s_V(\tau)$ obeys

$$\left(\frac{\partial}{\partial \tau} + ik_0 + \gamma/2\right)s_V(\tau) = -\gamma^{1/2}\phi(L-\tau), \quad \text{(A3)}$$

whose solution is

$$s_V(\tau) = \gamma^{1/2}\int_0^\tau d\tau'\phi(L-\tau')e^{-(ik_0+\gamma/2)(\tau-\tau')}$$

$$= \int_{-\infty}^L d\tau'\phi(\tau')\psi(L-\tau-\tau'). \quad \text{(A4)}$$

At $\tau = L$, this becomes $s_V(L) = \int_{-\infty}^L d\tau\,\phi(\tau)\psi(-\tau)$: the cavity acts as a filter, preferentially absorbing photons from the inverted mode $\psi^*(-\tau)$ and rejecting all others. Note that by making L large enough, essentially all of the photon in the mode $\psi^*(-z)$ can be absorbed: only an exponentially small portion $e^{-\gamma L}$ is missed. This inverted mode $\psi^*(-z)$ is precisely what the principal mode $\psi(z)$ is transformed into by the pulse inverter $\mathcal{I}$. In contrast, absorbed photons are reemitted into the principal mode. Long after absorbing a single photon, the cavity photon decays into the mode

$$\lim_{\tau\to\infty}\langle 0; z|e^{i\mathcal{H}_{\text{field}}\tau/\hbar c}e^{-i\mathcal{H}\tau/\hbar c}|1; \text{vac}\rangle = \psi(z-L). \quad \text{(A5)}$$

(Here, $|0; z\rangle = v_z^\dagger|0; \text{vac}\rangle$ and free-space translation has been removed by applying $e^{i\mathcal{H}_{\text{field}}\tau/\hbar c}$.)

We now summarize the PMP process. Before pulse inversion, the photon's mode function can be decomposed as $\alpha\psi(z) + \beta\psi_\perp(z)$ and as $\phi(z) = \alpha\psi_\perp^*(-z) + \beta\psi_\perp'(z)$ after inversion. The pulse propagates into the cavity through iris 1, which is initially open. Next, the cavity absorbs a portion of the pulse and rejects the rest. In order to prevent reflection of the rejected portion, iris 2 is initially closed. At time $\tau = L$,

the amplitude for the cavity to contain a single photon is α, i.e., the principal-mode photon has been transferred coherently to the cavity. At this point, iris 2 is opened (pulse timing is known) to allow the cavity photon to decay back into the principal mode, while iris 1 is shut in order to prevent further, unwanted absorption.

---

[1] I. L. Chuang and Y. Yamamoto, Phys. Rev. A **52**, 3489 (1995).

[2] T. B. Pittman, B. C. Jacobs, and J. D. Franson, Phys. Rev. A **64**, 062311 (2001).

[3] G. J. Milburn, Phys. Rev. Lett. **62**, 2124 (1989).

[4] Q. A. Turchette, C. J. Hood, W. Lange, H. Mabuchi, and H. J. Kimble, Phys. Rev. Lett. **75**, 4710 (1995).

[5] M. D. Lukin and A. Imamoğlu, Phys. Rev. Lett. **84**, 1419 (2000).

[6] L.-M. Duan and H. J. Kimble, Phys. Rev. Lett. **92**, 127902 (2004).

[7] K. Koshino, S. Ishizaka, and Y. Nakamura, Phys. Rev. A **82**, 010301 (2010).

[8] J. H. Shapiro, Phys. Rev. A **73**, 062305 (2006).

[9] J. H. Shapiro and M. Razavi, New J. Phys. **9**, 16 (2007).

[10] J. Gea-Banacloche, Phys. Rev. A **81**, 043823 (2010).

[11] P. L. Voss and P. Kumar, J. Opt. B: Quantum Semiclass. Opt. **6**, S762 (2004).

[12] K.-P. Marzlin, Z.-B. Wang, S. A. Moiseev, and B. C. Sanders, J. Opt. Soc. Am. B **27**, A36 (2010).

[13] M. Mašalas and M. Fleischhauer, Phys. Rev. A **69**, 061801 (2004).

[14] I. Friedler, G. Kurizki, and D. Petrosyan, Europhys. Lett. **68**, 625 (2004).

[15] Y.-F. Chen, C.-Y. Wang, S.-H. Wang, and I. A. Yu, Phys. Rev. Lett. **96**, 043603 (2006).

[16] I. Friedler, G. Kurizki, and D. Petrosyan, Phys. Rev. A **71**, 023803 (2005).

[17] I. Friedler, D. Petrosyan, M. Fleischhauer, and G. Kurizki, Phys. Rev. A **72**, 043803 (2005).

[18] A. André, M. Bajcsy, A. S. Zibrov, and M. D. Lukin, Phys. Rev. Lett. **94**, 063902 (2005).

[19] L. Vaidman, L. Goldenberg, and S. Wiesner, Phys. Rev. A **54**, R1745 (1996).

[20] N. Erez, Y. Aharonov, B. Reznik, and L. Vaidman, Phys. Rev. A **69**, 062315 (2004).

[21] G. A. Paz-Silva, A. T. Rezakhani, J. M. Dominy, and D. A. Lidar, Phys. Rev. Lett. **108**, 080501 (2012).

[22] H. Schmidt and A. Imamoğlu, Opt. Lett. **21**, 1936 (1996).

[23] M. Fleischhauer, A. Imamoğlu, and J. P. Marangos, Rev. Mod. Phys. **77**, 633 (2005).

[24] K. Koshino, Phys. Rev. A **80**, 023813 (2009).

[25] J.-Q. Liao and C. K. Law, Phys. Rev. A **82**, 053836 (2010).

[26] C. W. Gardiner and M. J. Collett, Phys. Rev. A **31**, 3761 (1985).

[27] J. H. Shapiro, IEEE J. Sel. Top. Quantum Electron. **15**, 1547 (2009).

[28] Because we consider a one-sided cavity, we should really only integrate over $k > 0$ in Eq. (4b). By using a truly linear dispersion relation, $\omega_k = ck$, we ensure that the unphysical, negative k modes are so far-detuned from the atomic system as to be irrelevant.

[29] K. Kojima, H. F. Hofmann, S. Takeuchi, and K. Sasaki, Phys. Rev. A **68**, 013803 (2003).

[30] B. H. Kolner and M. Nazarathy, Opt. Lett. **14**, 630 (1989).

[31] B. Kolner, IEEE J. Quantum Electron. **30**, 1951 (1994).

[32] M. T. Kauffman, Ph.D. thesis, Stanford University, 1994.

[33] O. Kuzucu, Y. Okawachi, R. Salem, M. A. Foster, A. C. Turner-Foster, M. Lipson, and A. L. Gaeta, Opt. Express **17**, 20605 (2009).

[34] M. A. Nielsen and I. L. Chuang, *Quantum Computation and Quantum Information* (Cambridge University Press, Cambridge, U.K., 2002).

[35] A. A. Houck, D. I. Schuster, J. M. Gambetta, J. A. Schreier, B. R. Johnson, J. M. Chow, L. Frunzio, J. Majer, M. H. Devoret, S. M. Girvin, and R. J. Schoelkopf, Nature (London) **449**, 328 (2007).

[36] C. Eichler, D. Bozyigit, C. Lang, L. Steffen, J. Fink, and A. Wallraff, Phys. Rev. Lett. **106**, 220503 (2011).

[37] D. Bozyigit, C. Lang, L. Steffen, J. M. Fink, C. Eichler, M. Baur, R. Bianchetti, P. J. Leek, S. Filipp, M. P. da Silva, A. Blais, and A. Wallraff, Nature Phys. **7**, 154 (2011).

[38] J. Schwartz, J. Azana, and D. Plant, *Proc. 2008 IEEE Radio and Wireless Symposium* (IEEE, Piscataway, 2008), pp. 487–490.

[39] J. Schwartz, I. Arnedo, M. Laso, T. Lopetegi, J. Azana, and D. Plant, IEEE Microwave Wireless Compon. Lett. **18**, 103 (2008).

[40] J.-T. Shen and S. Fan, Phys. Rev. Lett. **95**, 213001 (2005).

[41] O. Astafiev, A. M. Zagoskin, A. A. Abdumalikov, Y. A. Pashkin, T. Yamamoto, K. Inomata, Y. Nakamura, and J. S. Tsai, Science **327**, 840 (2010).